Philosophical Magazine,
Vol. 00, No. 00, DD Month 200x, 1–11

Three-dimensional model of martensitic transformations with elasto-plastic effects

Julia Kundin[a*], Heike Emmerich[a] and Johannes Zimmer[b]

[a] *Computational Materials Engineering (CME), Institute for Minerals Engineering, Center for Computational Engineering Science, Jülich-Aachen Research Alliance, RWTH Aachen University, DE-52056 Aachen, Germany*;
[b] *Department of Mathematical Sciences, University of Bath, Bath BA2 7AY, United Kingdom*

(v.1 released April 2008)

Martensitic transformations with elasto-plastic effects caused by the formation of dislocations in a parent austenite phase are studied by using a phase-field description. The method presented in this paper extends an existing microelastic model for the simulation of coherent martensitic transformations by taking into account the dislocation dynamics. Computational results show the difference between coherent and partially coherent martensitic transformation and illuminate elasto-plastic effects of transformation dislocations on the final martensitic microstructure.

1 Introduction

Martensitic transformations (MT) are phase transformations in solid materials where the coexistence of several stable orientation variants of martensite below the critical temperature genuinely leads to the formation of complex microstructure, which crucially determines macroscopic properties.

These phase transformations are often accompanied by elastic deformations due to structural changes and stresses at the boundaries between adjacent phases. The influence of the elastic effects on the transformation kinetics and the final form of the microstructure has been thoroughly investigated. Notably, an efficient method for the computer simulation of microstructure formation during a phase transformation was developed recently by Chen, Wang and Khachaturyan [1], as well as by Wang and Khachaturyan [2]. This approach integrates microelasticity into the phase-field theory. The method has been extended to investigate martensitic transformations in single crystals [3] and polycrystalline systems [4], and to investigate the effect of applied stress on the MT in such systems. All these studies concern coherent transformations and do not include effects of transformation dislocations, which genuinely occur during the semicoherent and partially coherent martensitic transformation and cause irreversible plastic changes in solid phases. The investigation of the formation of dislocations and their effects on the kinetics of phase transformations and on major characteristics of the final microstructure of martensite is of great interest; one motivation is that many materials that belong to this class, e.g., Fe-Ni alloys. Another reason is that the mobility of interfaces is decisive for the formation and evolution of microstructure, while in turn this mobility crucially depends on the presence and influence of dislocations at the interface. This is the topic of the present study, where we analyse the transformation of a cubic austenitic phase and tetragonal martensitic variants.

This study presents an extension of the cited phase-field model of martensitic transformation which explicitly takes into account the transformation-induced elastic strain during coherent phase transformations to the more common case of elasto-plastic problems where transformation dislocations form on the martensite/austenite interface. For this purpose, we have developed a description of eigenstrains of transformation dislocations and their elastic fields. Specifically, we formulate phase-field functions of dislocations of various orientational variants, which are formed in the parent austenite phase and move with the interface between adjacent phases. The coupling of the dislocation eigenstrain with the composition eigenstrain and also the dislocation phase-field functions with phase-field functions describing the phase transformation gives rise

*Corresponding author. Email: kundin@ghi.rwth-aachen.de

Philosophical Magazine
ISSN 1478-6435 print/ISSN 1478-6443 online
http://www.tandf.co.uk/journals
DOI: 10.1080/1478643YYxxxxxxxx

to a multiterm integro-differential kinetic equation for the simulation of martensitic transformations with dislocation effects.

Phase-field functions describing a system of dislocations were defined earlier in a number of papers. Koslowski *et al.* [5] formulated a phase-field theory of dislocation dynamics for an arbitrary number and arrangement of dislocation lines based on energy minimization. This theory builds on the phase-field model of Ortiz and Stainier [6], which is restricted to a single dislocation loop. At the same time, a phase-field model of the evolution of a dislocation system based on the Ginzburg-Landau kinetic equations was developed by Wang *et al.* [7]. They also discuss the possibility of extending the microelastic phase-field model of martensitic transformation by a phase-field model of the evolution of dislocations. In this case, the need of the solution of a system of kinetic equations becomes apparent. In this article, we propose and implement a model that combines a phase-field model for martensitic transformations with dislocations dynamics. For simplicity and efficient computability, we focus on the important case of transformation dislocations; thus, unlike for an elastic-plastic model with a full set of elastic and plastic (dislocation) phase-field functions, we do not need to simulate the dislocation dynamics by kinetic equations, because the transformation dislocations move with the martensite/austenite interface and the phase-field dislocation functions can be direct evaluated from the phase-field function of the martensite phase.

This paper is organised as follows. We introduce the model of dislocation elastic fields in Section 2, and subsequently give a formulation of the elastic problem as a coupling of the dislocation and composition eigenstrains in Section 3. A description of the phase-field kinetic equation including the elastic problem with dislocations can be found in Section 4. In Section 5 the numerical simulations of the time evolution and the final martensitic structure with elasto-plastic effects are presented and discussed.

2 Model of dislocation elastic fields

The general analytic theory of the elastic field of a dislocation is developed in many studies [8–13]. In this section, we describe a phase-field model of the transformation dislocations, which occur at the austenite/martensite interface.

A structural state of the austenite/martensite mixture is described by a set of continuous order parameters or *phase-field functions* $\{\phi_p(\vec{r})\} = (\phi_1(\vec{r}), \dots, \phi_\nu(\vec{r}))$, where $\vec{r}$ is the coordinate vector and ν is the total number of martensitic orientational variants. All phase-field functions change in an interval from 0 to ϕ_0 and the sum of this functions, including the austenitic phase, on a site $\vec{r}$ should be equal to ϕ_0, where we think of ϕ_0 as the value of the order parameter denoting the equilibrium stress-free state of martensite. The phase field function of austenitic phase is denoted $\phi^a(\vec{r}) = \phi_0 - \sum_{p=1}^{\nu} \phi_p(\vec{r})$. Analogously, we describe below the dislocation field by a dislocation phase-field function.

We consider an edge dislocation with Burgers vector $\vec{b}^{(p)}$ and slip plane with normal $\vec{n}^{(p)}$ in a Cartesian coordinate system defined by the cubic lattice of the parent austenitic phase, where $p \in \{1, \dots, \nu\}$ is an index corresponding to an orientational variant of the martensitic phase. The illustration of an edge dislocation with all constitual vectors is presented in the Fig. 1. Let the eigenstrain vector of an edge dislocation be given by

$$u_i^d(p, \vec{r}, \vec{r}_0) = b_i^{(p)} H(\vec{n}^{(p)} \Delta\vec{r}) H(-\vec{e}^{(p)} \Delta\vec{r}), \tag{1}$$

where $H(x)$ is the Heaviside step function, $\Delta\vec{r} = \vec{r} - \vec{r}_0$ with a site $\vec{r}_0$ located on the dislocation line, and $\vec{n}^{(p)}\Delta\vec{r}$ and $\vec{e}^{(p)}\Delta\vec{r}$ are scalar vector multiplications. The displacement $u_i^d(p, \vec{r}, \vec{r}_0)$ is caused by the relative slip $\vec{b}^{(p)}$ on the half plane ($\vec{n}^{(p)}\Delta\vec{r} = 0$, $\vec{e}^{(p)}\Delta\vec{r} < 0$) in the direction of $\vec{e}^{(p)} = \vec{b}^{(p)}/b^{(p)}$ along the Burgers vector, which is perpendicular to a dislocation plane.

In linear elasticity, the strain tensor is given by

$$\epsilon_{ij} = \frac{1}{2}\left(\frac{\partial u_i}{\partial r_j} + \frac{\partial u_j}{\partial r_i}\right). \tag{2}$$

By substituting (1) in (2), one can see that the eigenstrain tensor of an edge dislocation is of the form

$$\epsilon^d_{ij}(p,\vec{r},\vec{r}_0) = \frac{1}{2}\left(b_i^{(p)}n_j^{(p)} + b_j^{(p)}n_i^{(p)}\right)\delta(\vec{n}^{(p)}\Delta\vec{r})H(-\vec{e}^{(p)}\Delta\vec{r}) - \frac{1}{2}\left(b_i^{(p)}e_j^{(p)} + b_j^{(p)}e_i^{(p)}\right)\delta(\vec{e}^{(p)}\Delta\vec{r})H(\vec{n}^{(p)}\Delta\vec{r}), \quad (3)$$

where $\delta(x)$ is the Dirac delta function. This relation becomes an eigenstrain obtained by Mura [13] in the case $\vec{b} \parallel \vec{x}$, $\vec{n} \parallel \vec{y}$ and $\vec{r}_0 = 0$:

$$\epsilon^*_{12}(\vec{r}) = \frac{1}{2}b\delta(y)H(-x). \quad (4)$$

Since we are interested in the homogeneous strain associated with dislocations, we assume for now a periodic distribution of dislocations in the simulation domain of size $N_x \times N_y \times N_z$. Since a dislocation line is parallel to the vector $\vec{l}^{(p)} = \left[\vec{n}^{(p)} \times \vec{e}^{(p)}\right]$, we can choose a site s on the dislocation line that is located on a plane with normal vector $\vec{l}^{(p)}$ and passing through the centre of our coordinate system. The vector $\vec{r}_s$ representing the site s on a dislocation line can be chosen as a linear combination of the vectors $\vec{n}^{(p)}$, $\vec{e}^{(p)}$ and $\vec{l}^{(p)}$. Let L^d_b denote the average distance between dislocation lines in direction of $\vec{b}^{(p)}$, and similarly L^d_n and L^d_l for the directions determined by $\vec{n}^{(p)}$ and $\vec{l}^{(p)}$. Furthermore, in directions $\vec{n}^{(p)}$ and $\vec{l}^{(p)}$ the distance should be minimal in the limit of the discretisation cell width to integrate all positions on the dislocation plane. Then a vector $\vec{r}_s$ is calculated as a linear combination $\vec{r}_s = mL^d_n\vec{n}^{(p)} + nL^d_b\vec{e}^{(p)} + kL^d_l\vec{l}^{(p)}$, where m, n and k are integer values due to the crystalline nature. To take into account the stochastic nucleation of dislocations, the values n should be chosen randomly with an *a priory* assumed average distance L^d_b, which depends on the properties of the martensite transformation. This system of dislocations, we call "virtual" dislocations, becomes real only on the martensite/austenite interface.

As mentioned before, we restrict the analysis to dislocations at the interface between an austenitic and a martensitic phase, moving with the interface. For the eigenstrain tensor of a distribution of transformation dislocations we thus have

$$\epsilon^d_{ij}(p,\vec{r}) = \phi^a(\vec{r})\frac{\sum_s \phi^a(\vec{r}_s)\phi_p(\vec{r}_s)\epsilon^d_{ij}(p,\vec{r},\vec{r}_s)}{\sum_s \phi^a(\vec{r}_s)\phi_p(\vec{r}_s)}, \quad (5)$$

where the phase-field function of the austenitic phase $\phi^a(\vec{r})$ appears because the dislocations occur only in the austenitic phase and the multiplication $\phi^a(\vec{r}_s)\phi_p(\vec{r}_s)$ is responsible for the fact that the dislocation line (or the dislocation core) is located at the austenite/martensite interface and moves with the interface during the martensite transformation.

After the inserting (3) in (5), we see that the eigenstrain tensor of dislocations can be written in the form

$$\epsilon^d_{ij}(p,\vec{r}) = \epsilon^{0d(n)}_{ij}(p)\phi^a_p(\vec{r})\phi^{d(n)}_p(\vec{r}) + \epsilon^{0d(e)}_{ij}(p)\phi^a_p(\vec{r})\phi^{d(e)}_p(\vec{r}), \quad (6)$$

where $\epsilon^{0d(n)}_{ij}(p)$ and $\epsilon^{0d(e)}_{ij}(p)$ are given by

$$\epsilon^{0d(n)}_{ij}(p) = \frac{1}{2}\left(b_i^{(p)}n_j^{(p)} + b_j^{(p)}n_i^{(p)}\right)$$

and

$$\epsilon_{ij}^{0d(e)}(p) = -\frac{1}{2}\left(b_i^{(p)}e_j^{(p)} + b_j^{(p)}e_i^{(p)}\right), \tag{7}$$

and $\phi_p^{d(n)}(\vec{r})$ and $\phi_p^{d(e)}(\vec{r})$ are phase-field functions of all dislocations of an orientation variant p in the simulation domain, which are defined from eq. (3) as

$$\phi_p^{d(n)}(\vec{r}) = \frac{\sum_s \phi^a(\vec{r}_s)\phi_p(\vec{r}_s)\delta(\vec{n}^{(p)}\Delta\vec{r}_s)H(-\vec{e}^{(p)}\Delta\vec{r}_s)}{\sum_s \phi_p(\vec{r}_s)\phi^a(\vec{r}_s)}$$

and

$$\phi_p^{d(e)}(\vec{r}) = \frac{\sum_s \phi^a(\vec{r}_s)\phi_p(\vec{r}_s)\delta(\vec{e}^{(p)}\Delta\vec{r}_s)H(\vec{n}^{(p)}\Delta\vec{r}_s)}{\sum_s \phi_p(\vec{r}_s)\phi^a(\vec{r}_s)}, \tag{8}$$

with $\Delta\vec{r}_s := \vec{r} - \vec{r}_s$. In this manner, thanks to the dislocation phase-field function, the transformation dislocations form loop-shaped dislocation lines around martensitic patterns and the structure of these loops is defined by a combination of the martensite/austenite phase-field functions. The dislocation can move and interact as described by the phase-field model of Wang *et al.* [7].

3 Strain energy of a multiphase composition with transition dislocations

In this section, we define the total strain energy. Following Khachaturyan [14], Wang and Khachaturyan [2] and Artemev, Jin and Khachaturyan [4], let us consider a coherent multiphase mixture with the local stress-free strain tensor $\epsilon_{ij}^0(p,\vec{r}) = \epsilon_{ij}^{00}(p)\phi_p(\vec{r})$ reflecting the compositional inhomogeneity. The local stress-free strain tensor caused by dislocations was derived in the previous section (see eq. (6)) and is denoted $\epsilon_{kl}^d(p,\vec{r})$.

We write $\epsilon_{ij}(\vec{r})$ to denote the total strain. Then Hooke's low gives the local elastic stress

$$\sigma_{ij}^{el}(\vec{r}) = \lambda_{ijkl}\left[\epsilon_{ij}(\vec{r}) - \sum_{p=1}^{\nu}\left(\epsilon_{ij}^0(p,\vec{r}) + \epsilon_{kl}^d(p,\vec{r})\right)\right]. \tag{9}$$

The mechanical equilibrium give the set of equations

$$\sum_{j=1}^{3}\frac{\partial\sigma_{ij}^{el}(\partial\vec{r})}{r_j} = 0. \tag{10}$$

Since analytic solutions of such equations can be obtained for the strain distribution of a macroscopically homogeneous but microscopically (structurally) inhomogeneous body [14], it is reasonable to decompose the total strain $\epsilon_{ij}(\vec{r})$ as a sum of homogeneous and heterogeneous strains,

$$\epsilon_{ij}(\vec{r}) = \bar{\epsilon}_{ij} + \delta\epsilon_{ij}(\vec{r}), \tag{11}$$

such that $\int_V \delta\epsilon_{ij}(\vec{r})dV = 0$. The homogeneous strain is equal to the sum of the composition strain and the

dislocation strain (6),

$$\bar{\epsilon}_{ij} = \bar{\epsilon}_0 + \bar{\epsilon}_d = \sum_{p=1}^{\nu} \epsilon_{ij}^{00}(p) \frac{1}{V} \int_V \phi_p(\vec{r}) dV + \sum_{p=1}^{\nu} \epsilon_{ij}^{0d(n)}(p) \frac{1}{V} \int_V \phi_p^a(\vec{r}) \phi_p^{d(n)}(\vec{r}) dV + \sum_{p=1}^{\nu} \epsilon_{ij}^{0d(e)}(p) \frac{1}{V} \int_V \phi_p^a(\vec{r}) \phi_p^{d(e)}(\vec{r}) dV, \quad (12)$$

where V is the total volume of the system.

We now turn our attention to the heterogeneous displacement. Let us write $u_k(\vec{r})$ for the kth component of the displacement, related to the heterogeneous strain via the formula

$$\delta\epsilon_{ij} = \frac{1}{2} \left(\frac{\partial u_i}{\partial r_j} + \frac{\partial u_j}{\partial r_i} \right). \quad (13)$$

In order to find the heterogeneous displacement, one has to substitute equations (9), (11) and (13) into the mechanical equilibrium equations (10) and obtains

$$\lambda_{ijkl} \frac{\partial^2 u_k(\vec{r})}{\partial r_j \partial r_l} = \sum_{p=1}^{\nu} \sigma_{ij}^{00}(p) \frac{\partial \phi_p(\vec{r})}{\partial r_j} + \sum_{p=1}^{\nu} \left[\sigma_{ij}^{0d(n)}(p) \frac{\partial \left(\phi_p^a(\vec{r}) \phi_p^{d(n)}(\vec{r}) \right)}{\partial r_j} + \sigma_{ij}^{0d(e)}(p) \frac{\partial \left(\phi_p^a(\vec{r}) \phi_p^{d(e)}(\vec{r}) \right)}{\partial r_j} \right], \quad (14)$$

where λ_{ijkl} are the elastic constants, $\sigma_{ij}^{00}(p) := \lambda_{ijkl} \epsilon_{kl}^{00}(p)$, $\sigma_{ij}^{0d(n)}(p) := \lambda_{ijkl} \epsilon_{kl}^{0d(n)}(p)$, and $\sigma_{ij}^{0d(e)}(p) := \lambda_{ijkl} \epsilon_{kl}^{0d(e)}(p)$ are the elastic stresses. This equation can be solved in Fourier space, and one then finds

$$u_k(\vec{k}) = -\mathrm{i} \sum_{p=1}^{\nu} G_{ik}(\vec{k}) \cdot \cdot \left[\sigma_{ij}^{00}(p) \widehat{\phi}_p(\vec{k}) + \sigma_{ij}^{0d(n)}(p) \left(\widehat{\phi}_p^a * \widehat{\phi}_p^{d(n)} \right)(\vec{k}) + \sigma_{ij}^{0d(e)}(p) \left(\widehat{\phi}_p^a * \widehat{\phi}_p^{d(e)} \right)(\vec{k}) \right] k_j, \quad (15)$$

where $G_{ik}(\vec{k})$ is the Green tensor which is inverse to $G_{ik}^{-1}(\vec{k}) = k^2 \lambda_{ijkl} e_j e_l$, $\vec{e} = \vec{k}/k$ is the unit vector along the wave vector $\vec{k}$ and i denotes the imaginary unit. Furthermore $\widehat{\phi}_p(\vec{k})$ and $\widehat{\phi}_p^d(\vec{k})$ denote Fourier transforms, and the notation $(f * g)$ stands for a convolution of the functions f and g.

Then we can find the heterogeneous strain in the Fourier space as

$$\delta\epsilon_{ij}(\vec{k}) = \frac{\mathrm{i}}{2} \left(u_i(\vec{k}) k_j + u_j(\vec{k}) k_i \right). \quad (16)$$

The total elastic energy is given by

$$E_{\mathrm{elast}}^{\mathrm{tot}} = \frac{1}{2} \int_V \lambda_{ijkl} \epsilon_{ij}(\vec{r}) \epsilon_{kl}(\vec{r}) dV + E_0, \quad (17)$$

where E_0 measures the difference between the stress free state and the unstrained state,

$$E_0 = \frac{V}{2}\sum_{t,u=1}^{3}\sum_{p=1}^{\nu}\lambda_{ijkl}\epsilon_{ij}^{0(t)}(p)\epsilon_{kl}^{0(u)}(p)\left\langle\phi_p^{(t)}(\vec{r})\phi_p^{(u)}(\vec{r})\right\rangle; \tag{18}$$

we write $\langle\cdot\rangle$ to represent the average over the entire volume and $\sum_{t,u}$ for the sum over three types of elastic fields: the composition eigenstrain $\epsilon_{ij}^{00}(p)$ and the two eigenstrains of dislocations $\epsilon_{ij}^{0d(n)}(p)$ and $\epsilon_{ij}^{0d(e)}(p)$ (see eq. (6)). To express this conveniently in formulae, we use the indices t, u and write $\epsilon_{ij}^{0(1)} := \epsilon_{ij}^{00}$, $\epsilon_{ij}^{0(2)} := \epsilon_{ij}^{0d(n)}$, $\epsilon_{ij}^{0(3)} := \epsilon_{ij}^{0d(e)}$. Equation (18) generalises the corresponding dislocation-free formula (see, e.g., [4, Equation (11)]) via the inclusion of dislocation strains.

Substituting eq. (11) into eq. (17) and taking into account that by definition $\int_V \delta\epsilon_{ij}(\vec{r})dV = 0$, we have

$$E_{\text{elast}}^{\text{tot}} = \frac{V}{2}\lambda_{ijkl}\overline{\epsilon}_{ij}\overline{\epsilon}_{kl} + \frac{1}{2}\int_V \lambda_{ijkl}\delta\epsilon_{ij}(\vec{r})\delta\epsilon_{kl}(\vec{r})dV + E_0, \tag{19}$$

where the first term on the right side is the homorelaxation energy $E_{\text{relax}}^{\text{homo}}$ and the second term is the heterorelaxation energy $E_{\text{relax}}^{\text{hetero}}$. Substituting eqs. (12) and (16) into eq. (19) we obtain

$$E_{\text{relax}}^{\text{homo}} = -\frac{V}{2}\sum_{t,u=1}^{3}\sum_{p,q=1}^{\nu}\lambda_{ijkl}\epsilon_{ij}^{0(t)}(p)\epsilon_{kl}^{0(u)}(q)\left\langle\phi_p^{(t)}(\vec{r})\right\rangle\left\langle\phi_q^{(u)}(\vec{r})\right\rangle, \tag{20}$$

and

$$E_{\text{relax}}^{\text{hetero}} = -\frac{1}{2}\sum_{t,u=1}^{3}\sum_{p,q=1}^{\nu}\int B_{pq}^{tu}(\vec{e})\widehat{\phi}_p^{(t)}(\vec{k})\widehat{\phi}_q^{(u)*}(\vec{k})\frac{d^3\vec{k}}{(2\pi)^3}, \tag{21}$$

where $\{\cdot\}^*$ denotes the complex conjugate of $\{\cdot\}$, t, u are indices as above and we abbreviate by writing $\widehat{\phi}_p^{(1)}(\vec{k}) := \widehat{\phi}_p(\vec{k})$, $\widehat{\phi}_p^{(2)}(\vec{k}) := \left(\widehat{\phi}_p^a * \widehat{\phi}_p^{d(n)}\right)(\vec{k})$, and $\widehat{\phi}_p^{(3)}(\vec{k}) := \left(\widehat{\phi}_p^a * \widehat{\phi}_p^{d(e)}\right)(\vec{k})$ for the Fourier transforms of the phase-field functions. The coefficients $B_{pq}^{(tu)}(\vec{e})$ are given by the formula

$$B_{pq}^{tu}(\vec{e}) = e_i\sigma_{ij}^{0(t)}(p)\Omega_{ij}(\vec{e})\sigma_{kl}^{0(u)}(q)e_l, \tag{22}$$

with the stress tensors introduced above abbreviated as $\sigma_{ij}^{0(t)}(p) := \lambda_{ijkl}\epsilon_{ij}^{0(t)}$ for $t \in \{1, 2, 3\}$, and the Green tensor $\Omega_{ij}(\vec{e})$, which is inverse to the tensor $\Omega_{ij}^{-1}(\vec{e}) = \lambda_{ijkl}e_je_l$. Again, the expressions eq. (20) and eq. (21) differ from the dislocation-free setting (e.g., [4, Equations (8) and (9)] by the inclusion of the sum over t and u.

4 The phase-field kinetic equation

The dynamics of a single non-conserved phase-field function $\phi_p(\vec{r}, t)$ is governed by the Time-Dependent Ginzburg-Landau (TDGL) equation [15]. Following [2], we get the dynamics of a system of phase-field functions as

$$\frac{\partial\phi_p}{\partial t} = -\sum_{q=1}^{\nu}L_{pq}\frac{\delta F[\phi_q]}{\delta\phi_q} + \xi_p(\vec{r}, t), \tag{23}$$

where the indexes $p, q = 1, 2, 3$ denote orientational variants, $L_{pq} = L\delta_{pq}$ is the kinetic coefficient, F is the free energy functional and $\xi_p(\vec{r}, t)$ is the Langevin noise term which is Gaussian distributed [16]:

$$\left\langle \xi_p(\vec{r}, t)\xi_p(\vec{r}', t')\right\rangle = 2k_B T L\delta(\vec{r} - \vec{r}')\delta(t - t'). \tag{24}$$

The free energy functional F combines a chemical term and the elastic term of eq. (17). The chemical energy is

$$E_{\text{chem}} = \int_V \left[\frac{1}{2}\sum_{p=1}^{\nu} W^2 \frac{\partial^2 \phi_p(\vec{r})}{\partial r_i \partial r_j} + f_0(\{\phi_p(\vec{r})\})\right] dV, \tag{25}$$

where f_0 is the specific chemical energy of the transformation and W is the width of the interface.

Following [4], we write the kinetic equation (23) in a reduced form and measure all energies in the units of the transformation driving force $\Delta f = |f_0(\phi_0, 0, 0) - f_0(0, 0, 0)|$.

To simplify the expression, we write only one term of the dislocation eigenstrain, namely every expression involving $\epsilon_{kl}^{0d(n)}$, and suppress the analogous expressions involving $\epsilon_{kl}^{0*d(e)*}$. The terms in lines two and three originate from E_0, see eq. (18), the expressions in lines four to six stem from $E_{\text{relax}}^{\text{homo}}$ defined in (20), and lines seven to nine are due to $E_{\text{relax}}^{\text{hetero}}$ from (21). We use that $\lambda_{ijkl} = \lambda_{klij}$.

$$\begin{aligned}
\tau_\phi \frac{\partial \phi_p(\vec{r}, t)}{\partial t} &= W^2 \frac{\partial^2 \phi_p(\vec{r})}{\partial r_i \partial r_j} - \frac{\partial f_0^*(\{\phi_p(\vec{r})\})}{\partial \phi_p(\vec{r})} \\
&- \zeta\lambda_{ijkl}\epsilon_{ij}^{00}(p)\epsilon_{kl}^{00}(p)\phi_p(\vec{r}) - \zeta\lambda_{ijkl}\epsilon_{ij}^{00}(p)\epsilon_{kl}^{0d(n)}(p)\left[\phi^a(\vec{r}) - \phi_p(\vec{r})\right]\phi_p^{d(n)}(\vec{r}) \\
&+ \zeta\lambda_{ijkl}\epsilon_{ij}^{0d(n)}(p)\epsilon_{kl}^{0d(n)}(p)\phi_p^a(\vec{r})\phi_p^{d(n)}(\vec{r})^2 \\
&+ \zeta\lambda_{ijkl}\epsilon_{ij}^{00}(p)\sum_{q=1}^{\nu}\epsilon_{kl}^{00}(q)\left\langle\phi_q(\vec{r})\right\rangle + \zeta\lambda_{ijkl}\epsilon_{ij}^{00}(p)\sum_{q=1}^{\nu}\epsilon_{kl}^{0d(n)}(q)\left\langle\phi^a(\vec{r})\phi_q^{d(n)}(\vec{r})\right\rangle \\
&- \zeta\lambda_{ijkl}\epsilon_{ij}^{0d}(p)\phi_p^{d(n)}(\vec{r})\sum_{q=1}^{\nu}\epsilon_{kl}^{00}(q)\left\langle\phi_q(\vec{r})\right\rangle \\
&- \zeta\lambda_{ijkl}\epsilon_{ij}^{0d(n)}(p)\phi_p^{d(n)}(\vec{r})\sum_{q=1}^{\nu}\epsilon_{kl}^{0d(n)}(q)\left\langle\phi_q^a(\vec{r})\phi_q^{d(n)}(\vec{r})\right\rangle \\
&+ \zeta\sum_{q=1}^{\nu}\int B_{pq}^{00}(\vec{e})\widehat{\phi}_q(\vec{k})e^{\mathrm{i}\vec{k}\vec{r}}\frac{d^3\vec{k}}{(2\pi)^3} + \zeta\sum_{q=1}^{\nu}\int B_{pq}^{0d(n)}(\vec{e})\left(\widehat{\phi}^a * \widehat{\phi}_q^{d(n)}\right)(\vec{k})e^{\mathrm{i}\vec{k}\vec{r}}\frac{d^3\vec{k}}{(2\pi)^3} \\
&- \zeta\phi_p^{d(n)}(\vec{r})\sum_{q=1}^{\nu}\int B_{pq}^{0d(n)}(\vec{e})\widehat{\phi}_q(\vec{k})e^{\mathrm{i}\vec{k}\vec{r}}\frac{d^3\vec{k}}{(2\pi)^3} \\
&- \zeta\phi_p^{d(n)}(\vec{r})\sum_{q=1}^{\nu}\int B_{pq}^{d(n)d(n)}(\vec{e})\left(\widehat{\phi}^a * \widehat{\phi}_q^{d(n)}\right)(\vec{k})e^{\mathrm{i}\vec{k}\vec{r}}\frac{d^3\vec{k}}{(2\pi)^3} \\
&+ \xi_p^*(\vec{r}, t),
\end{aligned} \tag{26}$$

where $f_0^* = f_0/\Delta f$, $\tau_\phi = 1/(L\Delta f)$ and $\zeta = 1/\Delta f$.

Note that in our derivation of eq. (26) we have used the following formal calculation for a convolution of

two Fourier transformations, e. g., $\widehat{\phi}^a$ and $\widehat{\phi}_p^{d(n)}$ (for the last line, we recall that $\phi^a(r) = (\phi_0 - \sum_{p=1}^{\nu} \phi_p(r))$),

$$\begin{aligned}
&\frac{\partial}{\partial \phi_p(\vec{r})} \left(\widehat{\phi}^a * \widehat{\phi}_p^{d(n)} \right) (\vec{k}) = \frac{\partial}{\partial \phi_p(\vec{r})} \int \widehat{\phi}^a(\vec{k} - \vec{g}) \widehat{\phi}_p^{d(n)}(\vec{g}) d\vec{g} \\
&= \frac{\partial}{\partial \phi_p(\vec{r})} \int \left[\int \phi^a(\vec{r'}) e^{\mathrm{i}(\vec{k}-\vec{g})\vec{r'}} d\vec{r'} \right] \widehat{\phi}_p^{d(n)}(\vec{g}) d\vec{g} \\
&= - \int \left[\int \delta(\vec{r'} - \vec{r}) e^{\mathrm{i}(\vec{k}-\vec{g})\vec{r'}} d\vec{r'} \right] \widehat{\phi}_p^{d(n)}(\vec{g}) d\vec{g} \\
&= - \int e^{\mathrm{i}(\vec{k}-\vec{g})\vec{r}} \widehat{\phi}_p^{d(n)}(\vec{g}) d\vec{g} = -\phi_p^{d(n)}(\vec{r}) e^{\mathrm{i}\vec{k}\vec{r}}.
\end{aligned} \tag{27}$$

The specific chemical energy is approximated by a Landau-type polynomial written in terms of phase-field variables [4],

$$f_0^*(\phi_1, \phi_2, \phi_3) = f_0^*(0,0,0) + \frac{a_1}{2} \sum_{p=1}^{\nu} \phi_p^2 - \frac{a_2}{3} \sum_{p=1}^{\nu} \phi_p^3 + \frac{a_3}{4} \left(\sum_{p=1}^{\nu} \phi_p^2 \right)^2, \tag{28}$$

where we have chosen the dimensionless parameters $a_1 = 0.02$, $a_2 = 2.0$, $a_3 = 1.0$. The function f_0^* attains the minima at $\phi_0 = 1.98$ (see, e.g., [4]).

5 Numerical simulations

We solve eq. (26) by a finite difference method. The transformation is calculated numerically with the Fast Fourier Transform (FFT) method. In order to reduce the oscillations in the solution of eq. (26) in Fourier space (see the work of Hu and Chen [17]), we suggest the use of the following approximation of the delta function in eq. (8) in the limit of a Cauchy distribution

$$\delta_\xi(x) = \frac{1}{\pi} \frac{\xi}{(x^2 + \xi^2)}. \tag{29}$$

Then we can use the approximation function

$$H_\xi(x) = \frac{1}{\pi} \arctan\left(\frac{x}{\xi}\right) + \frac{1}{2}, \tag{30}$$

for the Heaviside function, where $\xi \approx 2a_c$ is the width of the dislocation core in the cubic parent austenitic phase with crystal lattice parameter a_c.

We simulated the MT in a single-crystal parent phase system. The morphology of ferrous lath martensite is investigated in dependency on the transformation dislocation density. It is known that laths do not form as self-accommodating units (unlike the polytwinned martensite) and that leads to the preservation of retained austenite. For example, an Fe-20Ni-5Mn alloy produces individually nucleated laths [18,19] with relationships of the form $(111)_F||(101)_B$, and $[1\bar{1}0]_F|||[11\bar{1}]_B$, where thin films of retained austenite are observed. The similar relationship and lath structure is formed in Fe-(0.2-0.4)C carbon steels [20, 21]. We suggest that transformation dislocations accommodate the strain and lead to an increase of the final martensite fraction.

For simplicity we assume that the nucleation produces three orientational variants for the martensitic

phase with eigenstrains, containing only diagonal terms as for Fe-Ni alloys in [22],

$$\begin{aligned}
&\epsilon_1^{00}(1) = 0.1322, && \epsilon_2^{00}(1) = 0.1322, && \epsilon_3^{00}(1) = -0.1994,\\
&\epsilon_1^{00}(2) = 0.1322, && \epsilon_2^{00}(2) = -0.1994, && \epsilon_3^{00}(2) = 0.1322,\\
&\epsilon_1^{00}(3) = -0.1994, && \epsilon_2^{00}(3) = 0.1322, && \epsilon_3^{00}(3) = 0.1322.
\end{aligned} \tag{31}$$

The Burgers vector for martensitic transformations can for example be assumed to be

$$b^T(1) = \frac{a_c}{6}\left\{1,1,\overline{2}\right\}, \qquad b^T(2) = \frac{a_c}{6}\left\{1,\overline{2},1\right\}, \qquad b^T(3) = \frac{a_c}{6}\left\{\overline{2},1,1\right\} \tag{32}$$

with corresponding slip planes

$$n^T(1) = n^T(2) = n^T(3) = \frac{1}{\sqrt{3}}\left\{1,1,1\right\}. \tag{33}$$

To estimate the averaged interdislocation distance L_b^d, we use a misfit on habitus planes, which correspond to the slip planes of the transformation dislocations (33). The misfit of a austenite/martensite interface can be defined from a difference in the lattice parameters on a habit plane in the direction of $\vec{b}^{(p)}$ as

$$\epsilon^{\text{misfit}} = 1 - \frac{\sqrt{2}}{2}\sqrt{\left(\frac{a}{a_c}\right)^2 + \left(\frac{c}{a_c}\right)^2}, \tag{34}$$

where a and c are the crystal parameters of the tetragonal stress-free martensite phase. A difference in the lattice parameters of the martensite and austenite phases can be derived from the eigenstrain of the martensite transformation (31), $a/a_c = 1 - 0.1322$, and $c/a_c = 1 + 0.1994$. Then the distances between dislocation planes is $L_b^d = a_c/\epsilon^{\text{misfit}} \backsimeq 84\ a_c$. This corresponds to the dislocation density $\rho = 5.0 \times 10^{10}$ cm^{-2} at $a_c = 4.5$ nm. But we should keep in mind that such an estimation of the interdislocation distance does not correspond to the real conditions of the phase transformation.

In the present study, we use a cubic domain of the size N^3 with $N = 46\ \Delta x$, where we choose $l_c = 200$ nm for the capillary length and $\Delta x = l = l_c/4 = 50\ a_c$ for the discretisation cell width. The time increment is chosen as $\Delta t = 0.5$. The elastic constants are taken to be those of of a Fe-31 at. % Ni alloy, namely $c_{11} = 1.404 \times 10^{11}$ Pa and $c_{12} = 0.84 \times 10^{11}$ Pa [23]. The input parameters for the simulation are $\tau_\phi = 1.0$, $W = 4\ \Delta x$ and $\Delta f = 3.488 \times 10^8$ J m^{-3} [4].

The simulation was performed for various interdislocation distances $L_b^d == \{4, 6, 8, 10, 12\}\ \Delta x$ (for simplicity we use further the notation $L = L_b^d$). The case $L_b^d = 2\Delta x$ corresponds to our estimation of the mean interdislocation distance for the assumed input eigenstrains (31) according to eq. (34). As mentioned before, we generate the random distribution of dislocations in the simulated domain. Furthermore we assume here that the mean interdislocation distance does not change during the transformation and is defined only by crystallography and the relationship of a martensitic transformation, although in real systems it should increase due to the increasing stress in the austenitic phase.

The final fraction of the martensite phase λ was estimated after 120 time steps, where the steady state is reached. The nucleation of individual laths was simulated using the random noise defined in eq. (24) and was applied for the time interval $n\Delta t$. The nucleation rate was chosen as $n = 10, 20$ for the nuclei in the simulated domain. The mean size of martensite laths for n nuclei in the domain can be estimated as $\tilde{l} = N/n = \langle 230, 115\} a_c$.

In Fig. 2, the visualisation of the simulated microstructure as a two-dimensional cross-section is given for various interdislocation distances. The three orientational variants have different colours, while the austenite matrix is white. It can be seen that the volume fraction of the austenitic phase increases with L. The microstructure after 30 time steps is presented in Fig. 3 in a three-dimensional plot to show how the growing martensite laths of various orientations are distributed in the simulated domain. The structures

Table 1. Fitting parameters of simulated dependencies: martensite fractions vs. interdislocation distances for various input parameters (nucleation rate n and gradient energy coefficient W^{*2}).

	$n = 10$ $W^{*2} = 1.5$	$n = 20$ $W^{*2} = 1.5$	$n = 20$ $W^{*2} = 2$	$n = 20$ $W^{*2} = 3$
λ_0	0.7267	0.72563	0.7258	0.7260
L_0	107.8	107.8	107.8	107.8
α	0.0166	0.0167	0.0183	0.0187

obtained in the simulations was compared to the experimentally observed martensitic structures in [18, 19]. For a comparison we have also simulated the nucleation of the strain-accommodating polytwinned martensite structure (see Fig. 2 (e)). Here the retained austenite fraction is not visual due to the complete strain relaxation [4].

In Fig. 4 (a-d), the time evolution of the martensitic phases as a function of the interdislocation distance is shown. The effect of dislocations is very pronounced. The increase of the dislocation density affects the increase of the transformation velocity and the increase of the final martensite volume fraction. The change of the number of nuclei from $n = 10$ to $n = 20$ increases the growth velocity, but the final fraction of martensite changes less than 1% (Fig. 4 (a,b)). The change of the gradient energy coefficient to $W^{*2} = 2$ and $W^{*2} = 3$ affects the increase of the growth velocity, too (Fig. 4 (c,d)), the final fraction of martensite increases more than 2%.

In Fig. 5, the final martensite fraction for the three orientational variants as a function of interdislocation distance is illustrated. The fitting of simulated curves gives the following logarithmic description for the dependence of λ on L and dislocation density $\rho \propto 1/L^2$ with the correlation coefficient $R = 0.999$:

$$\lambda = \lambda_0 + \alpha \ln\left(\frac{L_0^2}{L^2} + 1\right) = \lambda_0 + \alpha \ln\left(\frac{\rho}{\rho_0} + 1\right); \tag{35}$$

here $\lambda_0(L = \infty) = 0.72669$ is the final volume fraction without dislocations, $\alpha = 0.01661$ is a dimensionless coefficient and $L_0 = 107.80\ \Delta x$ is a reference interdislocation distance, which corresponds to $\rho_0 = 1.6 \times 10^7$ cm^{-2} at $a_c = 4.5$ nm. These calculated parameters for various nucleation rates and gradient energy coefficients are presented in Table 1.

Eq. (35) can be simplified by the relation $\lambda = \lambda_0 + \alpha\rho^{1/2}$, which shows the dependence of the martensite fraction on the stress caused by dislocations $\tau \propto \rho^{1/2}$. The fitting of simulated curves by this relation gives a worse correlation with the coefficient $R = 0.876$. Note that the real dislocation density increases during the transformation due to the formation of new dislocations with the increasing length of martensite/austenite boundaries.

In summary, in this way, we found the engineering limits for dislocation effects on the martensitic transformation in steel. Simulation results demonstrate that the elastic interaction between martensite laths of various orientations and between martensite laths and dislocations imposes the decrease of the elastic energy and as a consequence causes the increase of the transformation velocity and the final fraction of martensite without visual changes in the microstructure and the habit of the martensitic phase.

In the future work we will investigate the real interdislocation distance, which can change during the martensitic transformation, via estimation of an energetic barrier for the dislocation formation. That can be useful for the investigation of martensitic transformation under applied stresses.

6 Conclusion

In this study, we presented a 3D phase-field model of martensitic transformations allowing for the formation of dislocations on the interface between adjacent phases. We have developed the description of elastic fields of dislocations through phase-field dislocation functions, which makes available effective tools derived from the phase-field theory of phase transformations with elasticity. The computer simulations for the model presented here are performed to shed some light on the plastic-elastic effects caused by transformation dislocations. The simulations have demonstrated the strong dependencies of the final martensite fraction

on the interdislocation distance. In a future work, we will investigate the real interdislocation distance via the estimation of an energetic barrier for the formation of dislocations. The model could be a tool for future computer simulations of martensitic transformations in real systems, where the available elastic and crystallographic data relating to the parent and martensitic phases are used as input data.

7 Acknowledgements

The authors would like to thank J. Hubert for valuable discussions and support and S. Cottenier for a critical reading of this manuscript. J. Z. gratefully acknowledges the financial support of the EPSRC through an Advanced Research Fellowship (GR / S99037 / 1). The Interactive Ideas Factory at the University of Bath, an EPSRC Bridging the Gaps project (EP / E018122 / 1) funded a visit of H. E. to the University of Bath.

References

[1] L.Q. Chen, Y. Wang and A.G. Khachaturyan, Phil. Mag. Lett. 65 (1992) p.15–23.
[2] Y. Wang and A.G. Khachaturyan, Acta Mater. 45 (1997) p.759–773.
[3] A. Artemev, Y.M. Jin and A.G. Khachaturyan, Acta Mater. 49 (2001) p.1165.
[4] A. Artemev, Y.M. Jin and A.G. Khachaturyan, Philos. Mag. A 82 (2002) p.1249–1270.
[5] M. Koslowski, A.M. Cuitiño and M. Ortiz, J. Mech. Phys. Solids 50 (2002) p.2597–2635.
[6] M. Ortiz and L. Stainier, Comput. Methods Appl. Mech. Engrg. 171(3-4) (1999) p.419–444.
[7] Y.U. Wang, Y.M. Jin, A. M. Cuitiño and A.G. Khachaturyan, Acta Mater. 49 (2001) p.1847–1857.
[8] J.W. Christian *The Theory of Transformation in Metals and Alloys*, Pergamon Press, Oxford, 1965.
[9] V.L. Indenbom and J. Lothe *Elastic Strain Fields and Dislocation Mobility*, Elsevier Science Ltd., New York, 1992.
[10] J.P. Hirth and J. Lothe *Theory of Dislocations*, Second John Wiley & Sons Inc., New York, 1982.
[11] R. Peierls, Proc. Phys. Soc. 52 (1940) p.34–37.
[12] F.R.N. Nabarro, Proc. Phys. Soc. 59 (1947) p.256–272.
[13] T. Mura *Micromechanics of Defects in Solids*, Kluwer Academic Publishers, Dordrecht, 1983.
[14] A.G. Khachaturyan *Theory of Structural Transformations in Solids*, J. Wiley and Sons, New York and London, 1983.
[15] J.P. Gunton, M. San Miguel and P.S. Sahni in *Phase Transitions and Critical Phenomena*, C. Domb and J.L. Lebowitz, eds., Academic Press, New York, 1983, p. 267.
[16] E.M. Lifshitz and L.P. Pitaevskii, 1980, Vol. 5, Statistical Physics. in *Landau and Lifshitz Course of Theoretical Physics* 3rd ed., Pergamon Press, Oxford.
[17] S.Y. Hu and L.Q. Chen, Acta Mater. 49 (2001) p.463–472.
[18] B.P.J. Sandvik and C.M. Wayman, Metall. Trans. 14A (1983) p. 809.
[19] K. Wakasa and C.M. Wayman, Acta Metall. 29 (1981), p.973.
[20] B.P.J. Sandvik and C.M. Wayman, Metallography. 16 (1983) p.199.
[21] M.A. Shtremel, Yu.G. Andreev, and D.A. Kozlov, Metal Science and Heat Treatment, 41(3 - 4) (1999) p. 140–145.
[22] J.E. Breedis and C.M. Wayman, Trans. AIME 224 (1962) p.1128–1133.
[23] G. Hausch and H. Warlimont, Acta Metall. 21 (1973) p.401–414.

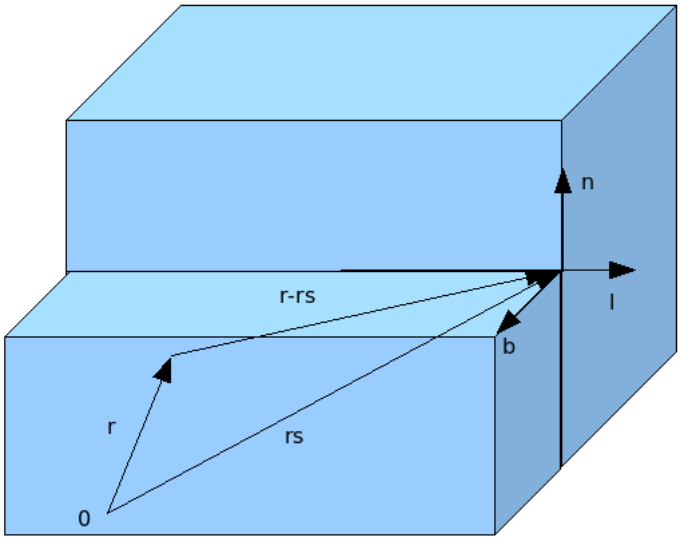

Figure 1. Schematic illustration of an edge dislocation. Here, b is the Burgers vector, and n is the unit vector normal to the slip plane.

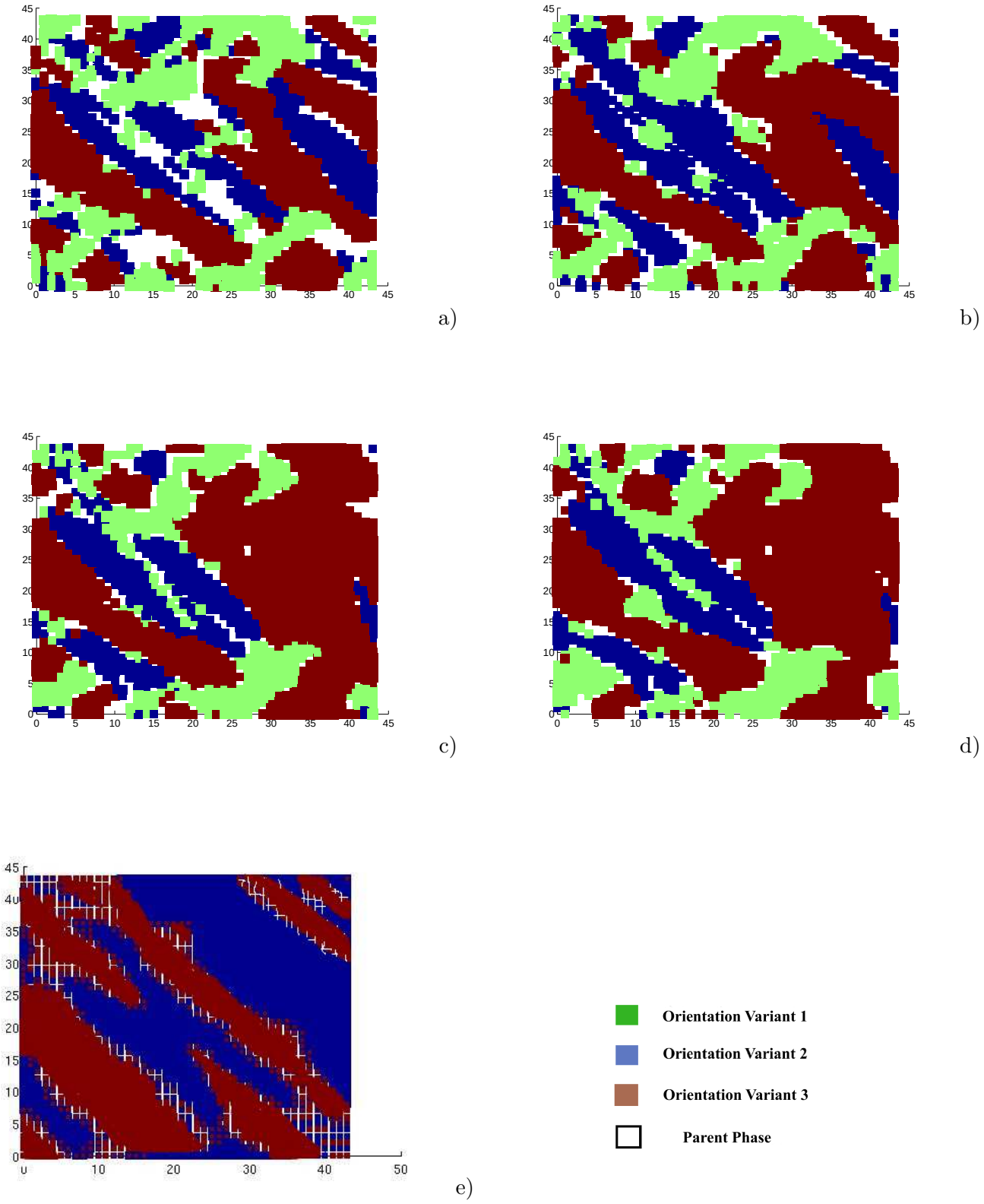

Figure 2. Martensitic structures for three orientational variations in two space dimensions, obtained without dislocations (a) and with dislocations at $L/\Delta x = 12$ (b), $L/\Delta x = 6$ (c) and $L/\Delta x = 4$ (d). The nucleation rate is $n = 10$.

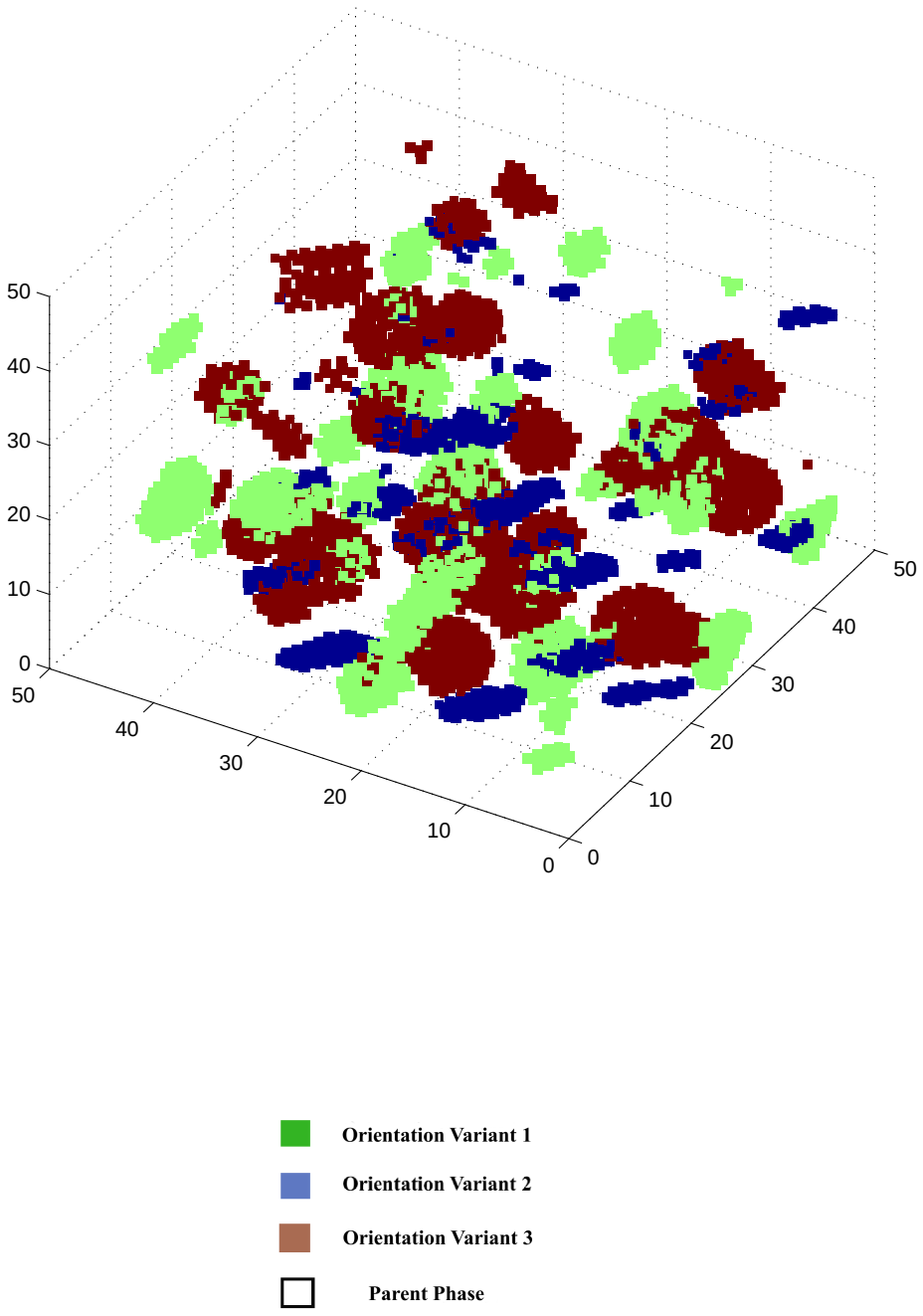

Figure 3. Martensitic structure for three orientational variations in three space dimensions, for a nucleation rate $n = 10$ and $t/\Delta t = 30$.

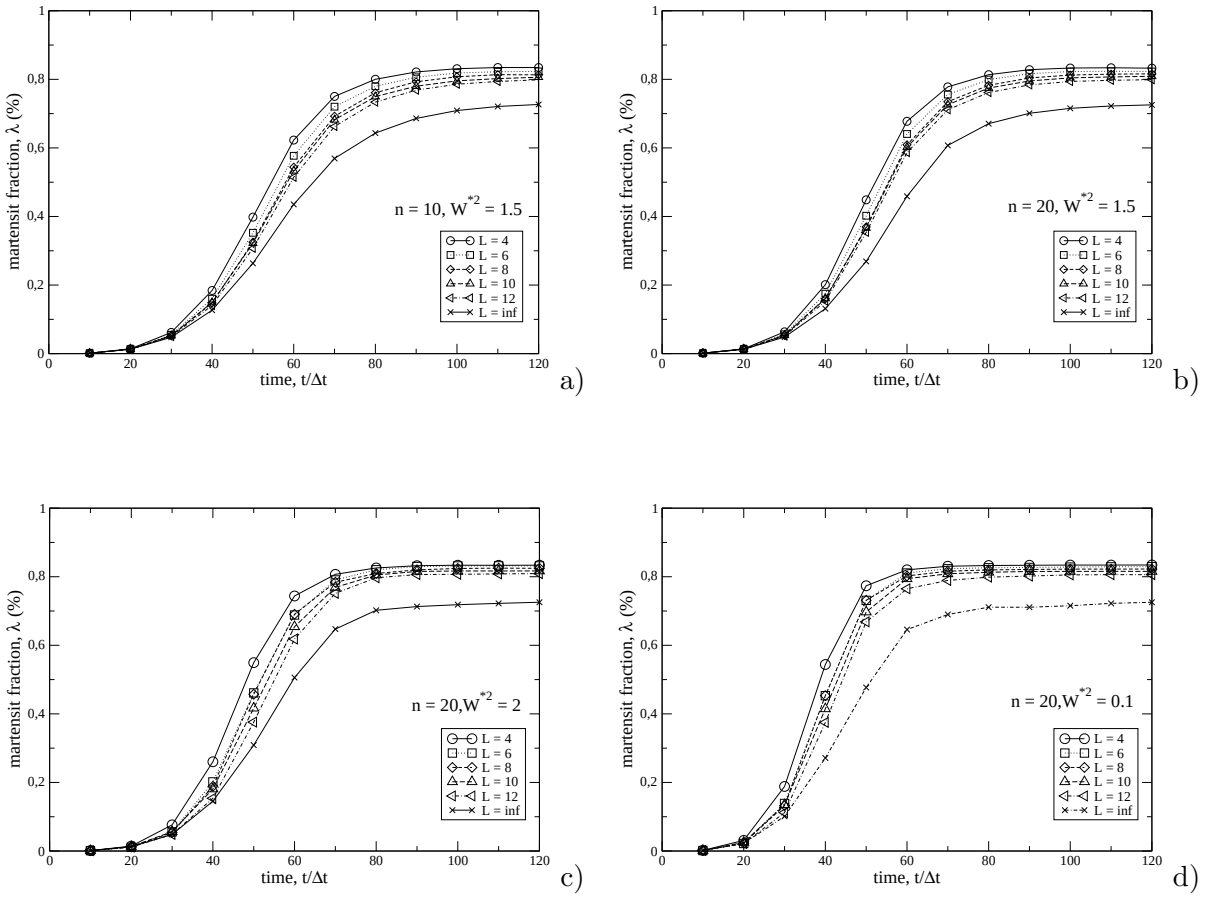

Figure 4. The time evolution of the martensite volume fraction of three orientational variants of martensite at various interdislocation distances. The nucleation rate is $n = 10$ (a) and $n = 20$ (b).

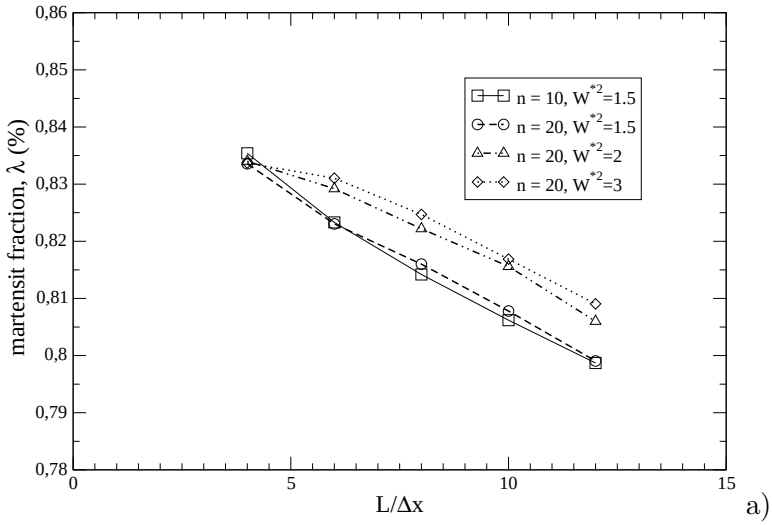

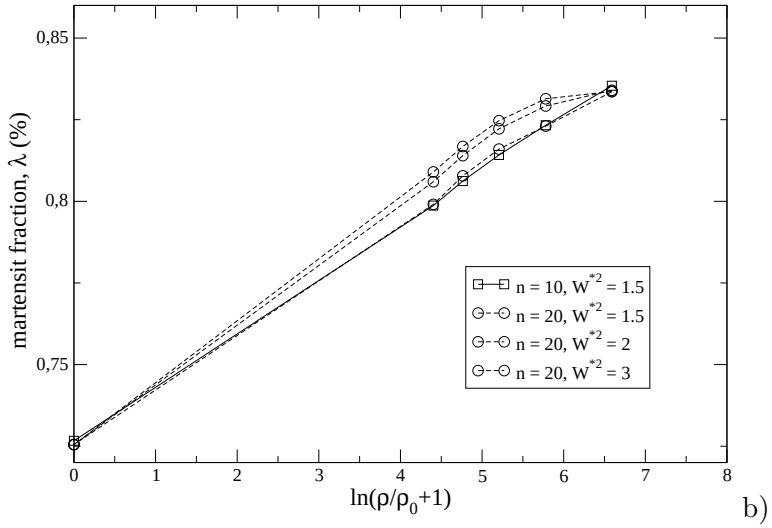

Figure 5. The martensite volume fraction of three orientational variants of martensite at the end of a transformation in dependency on the interdislocation distance in normal (a) and logarithmic (b) plots.